Journal of
Tissue Science & Engineering

Slimi and Mahjoubi, J Tissue Sci Eng 2019, 10:1
DOI: 10.4172/2157-7552.1000223

Research Article | Open Access

Enhancement of Displacement Estimation of Breast Tissue in Ultrasound Elastography

Taher Slimi[1*], Romaissa Tamali[2] and Halima Mahjoubi[1]

[1]*University of Tunis El Manar, Laboratory of Biophysics and Medical Technologies, High Institute of Medical Technologies, Tunis, Tunisia.*
[2]*University of Larbi Ben M'hidi, Oum El Bouaghi, Algeria.*

Abstract

Breast tissue displacements estimation in static ultrasound elastography, is a medical imaging technique which provides information on the local rigidity of tissues. Despite the fact that this technique has a major interest in clinical diagnosis, it suffers from increased deterioration due to the presence of speckle noise, artifacts and poor detail accuracy which appeared during the B-mode image acquisition process. Therefore, the application of Block Matching (BM) technique will greatly amplify the speckle noise and deteriorate the image quality. In this perspective, the implementation of an optimal technique is crucial for optimizing the quality of mammary displacements tissue. In this paper, we propose a new method based on the BM model that is to improve the old BM (OBM) technique. In this respect, an improvement of pre-processing step is satisfactory, in order to establish accurate tissue displacement estimation. The research was validated on a database of 20 patients with breast malignant tumor. Biophysical parameters has been adapted and used to eliminate artifacts and speckle noise, once the images are filtered; the BM model is implemented after to estimate tissue displacements. Based on the clinical results, quantitative analysis verifies that the tissue displacements estimated by our proposed strategy are more efficient than the OBM and Bilinear Deformable Block Matching (BDBM) techniques, our proposed approach gives better values in term of standard deviation (SD), higher contrast to noise ratio (CNR), greater peak signal-to-noise ratio (PSNR) and excellent structural similarity (SSIM) than OBM and BDBM techniques. The results of the proposed model are encouraging, allowing excellent estimates. The proposed model provides a new and appropriate solution for improving estimation of mammary tissue displacements. The proposed new strategy could be a powerful diagnostic tool to be used in clinical evaluation dedicated to breast ultrasound elastography.

Keywords: Breast ultrasound elastography; Biophysical parameters; Speckle noise; Displacement estimation

Abbreviations: BM: Block Matching; OBM: Old Block Matching; BDBM: Bilinear Deformable Block Matching; SD: Standard Deviation; CNR: Contrast to Noise Ratio; PSNR: Peak Signal-to-Noise Ratio; SSIM: Structural Similarity; ROI: Region of Interest; CC: Correlation Coefficient.

Introduction

Static ultrasound breast elastography has gradually developed over the years to become a sophisticated tool for the diagnosis of breast lesions. Thus, to distinguish the rigidity of mammary tumors, elastography is used to give information about tumors elasticity. It provides additional information on mammary lesions compared to conventional ultrasound and mammography [1].

Numerous studies have indicated that they can increase the specificity of conventional B-mode ultrasound image in the evaluation, characterization and differentiation of benign and malignant mammary masses [2]. With this technique, the acoustic information concerning the stiffness of the lesion is converted into a black and white or color image which can also be superimposed over B-mode images.

Mammary tumors are characterized by an increasing stiffness of the mammary tissue, indeed; the pathological changes of the mammary tissues are generally correlated with changes in the medium elasticity. Therefore, the tumor tissue stiffness could be a good diagnostic criterion useful for clinical evaluation [3].

On physical examination, it has long been recognized that mammary tumors tend to feel tough compared to non-tumor tissues. Breast elastography provides a non-invasive assessment of the stiffness or hardness of the mammary mass. Many data have been published suggesting that an association between the rigidity of mammary tissues and the onset of mammary tumors is biologically plausible [4].

Images of tissue displacements can be created by comparing ultrasound B-mode images obtained before and after slight tissue compression. In this respect, after compression by ultrasonic probe, the soft tissues deform more than the rigid tissues [5].

However, the utility of ultrasonic elastography is degraded by the presence of speckle noise in tissue displacements images. This type of noise is an inherent property of ultrasound medical imaging. It leads to decreasing the resolution and the contrast of the image which deteriorates the image quality, affects the interpretation and the diagnostic tasks of this imaging modality.

Therefore, speckle noise reduction is a crucial step in images pre-processing, whenever ultrasound elastography is used for medical imaging. So speckle noise suppression is a very important task and the image must be filtered, without affecting the important characteristics [6].

In the literature, several methods have been developed for

***Corresponding author:** Taher Slimi, Laboratory of Biophysics and Medical Technologies, High Institute of Medical Technologies of Tunis, University of Tunis El Manar, Zouhair Essafi Street, Tunis, Tunisia, Tel: 0021622352994; E-mail: slimi.taher@hotmail.com

Received March 14, 2019; **Accepted** March 27, 2019; **Published** April 04, 2019

Citation: Slimi T, Tamali R, Mahjoubi H (2019) Enhancement of Displacement Estimation of Breast Tissue in Ultrasound Elastography. J Tissue Sci Eng 9: 223. doi: 10.4172/2157-7552.1000223

Copyright: © 2019 Slimi T, et al. This is an open-access article distributed under the terms of the Creative Commons Attribution License, which permits unrestricted use, distribution, and reproduction in any medium, provided the original author and source are credited.

displacements estimation in ultrasonic elastography, those based on the BM technique, in spite of their slow calculation time they are the most common thanks to their availability in the ultrasound imaging modalities and their dispersion in other imaging modalities [7]. The in-depth analysis of the famous MB technique asserts that this method suffers from the diffusion of shimmer noise in the image of tissue displacements. Current advances in BM development technique require the use of speckle noise reduction techniques and the minimization of artifacts in the tissue displacement image [8].

In order to solve the problem of the appearance of noise and artifacts in estimating tissue displacements, several filtering methods have been proposed in the literature. These methods can be simply classified into five categories, namely the local adaptive filter, the anisotropic scattering filter, the multiscale filter, the non-local filter and the hybrid filter [9].

Since the above methods do not achieve an optimum balance between noise removal and detail preservation, it is desirable to seek a technique that improves the performance of a high filtering capacity and better edges preservation.

In this paper we propose a new approach that improves the classical BM technique that we call it here: OBM, the proposed new approach exploits the impact of the biophysical parameters combined with the BM model. The proposed method improves the OBM technique used in Breast tissue displacements.

The results of *in-vivo* studies are presented to evaluate the performance of the proposed method. We show that the proposed model has improved the OBM technique; also it has improved the diagnosis of malignant pathologies during the clinical evaluation.

The performance of our proposed method is compared with the OBM and BDBM approaches; we show that our proposed method is more accurate and more efficient. It gives better values in terms of SD, higher CNR, greater PSNR, and excellent SSIM than other methods.

This paper is organized as follows: the adapted biophysical approach and BM model theory of displacements estimation are resumed and presented in "Methods" section.

"Results" section shows the results on *in-vivo* breast images, we address also the comparison between the results obtained with our proposed method and those obtained with OBM and BDBM techniques. "Discussion" section shows the discussion of results. Concluding remarks are left to "Conclusion" section.

Methods

Biophysical image processing

The ultrasonic image is very degraded by the dominance of speckle noise, corresponding to multiple coherent reflections from the environment around the target [10]. The existence of speckle noise and artifacts induced by tissues displacements degrades the visual evaluation in ultrasound imaging [11]. In this case, the treatment of B-mode images becomes a crucial step in improving the quality of tissue displacements estimation. In this context, we can act on the biophysical parameters tools in order to reduce the speckle noise and artifacts with preservation of signal containing diagnostic information. Once the images are filtered, they will be injected into a displacement estimation algorithm.

Rejection: The rejection function parameter is a low pass spatial filter, which passes only the spatial frequencies less than or equal to its cut-off frequency integrated into the ultrasound device, it designed to bring out or suppress the speckle noise in the images by relying on their spatial frequencies. The spatial frequency is directly related to the texture of tissues, corresponding to the frequency variation of echogenicity in ultrasound image. Therefore, increasing the rejection parameter meaning decreasing the cut-off frequency of filter. Consequently, the parameterization of the cut-off frequency helps to reduce the noise and to maintain softening details, making the image less flickering and easier interpretation. As a result, the rejection function contributes to select only the high autocorrelation signals having a high SNR. It retains only the autocorrelation which has a high SNR corresponding to a noise-free image with more details representing the diagnostic information. As a result, low autocorrelation signals will be rejected since they contribute to providing poor quality images [12,13].

The convolution product of the B-mode image f (i,j) with a filter h(i,j) is given by:

$$f^{'}(i,j)=(f^{*}h)(i,j)=\sum_{n=1}^{N}\sum_{m=1}^{M}f(i,j)h(n-i,m-j) \qquad (1)$$

h is a square mask with d is the odd size, so the expression becomes:

$$f^{'}(i,j)=(f^{*}h)(i,j)=\sum_{n=-\frac{d-1}{2}}^{\frac{d-1}{2}}\sum_{m=-\frac{d-1}{2}}^{\frac{d-1}{2}}f(i,j)h(n-i,m-j) \qquad (2)$$

The transfer function H(u,v) of the low-pass filter is given by:

$$H(u,v)=\begin{cases}1 & if\ \sqrt{u^2+v^2}\le D_0\\ 0 & if\ \sqrt{u^2+v^2}>D_0\end{cases} \qquad (3)$$

Where D_0 is the cut-off frequency, this filter suppresses the frequency components having a radial frequency $\sqrt{u^2+v^2}$ higher than D_0.

Persistence: The persistence parameter is a low pass spatial filter; it has the same operating principle as rejection parameter, therefore, increasing the persistence meaning decreasing the cut-off frequency of filter. Consequently, the parameterization of the cut-off frequency helps to reduce the noise and to maintain softening details, making the image less flickering and easier interpretation. It is available in real time and in frozen mode [14,15].

The convolution product of the B-mode image $f^{'}$ (i,j) with a persistence filter g(i,j) is given by:

$$f^{''}(i,j)=(f^{'*}g)(i,j)=\sum_{n=-\frac{d-1}{2}}^{\frac{d-1}{2}}\sum_{m=-\frac{d-1}{2}}^{\frac{d-1}{2}}f^{'}(i,j)g(n-i,m-j) \qquad (4)$$

Where $f^{''}$ (i,j) is the result of applying persistence.

Smoothing: Smoothing parameter is a low pass spatial filter that it used in ultrasonic imaging as a pre-treatment step, it has the same operating principle as rejection function and persistence parameters, it used in order to produce a more homogeneous and smooth image, added to attenuate the speckle noise that is still present after the application of rejection and persistence parameters. In this perspective, the central pixel of the filter is replaced by the mean value of its neighborhood pixels. As a result, this operation consists most often of applying to the image a smoothing producing a soft B-mode image [16,17]. Increasing the smoothness parameter value decrease the cut-off frequency value and produces a smooth and filtered image which facilitates clinical interpretation.

The convolution product of the B-mode image f" (i,j) with a smoothing filter k(i,j) is given by:

$$f'''(i,j) = (f''*k)(i,j) = \sum_{n=-\frac{d-1}{2}}^{\frac{d-1}{2}} \sum_{m=-\frac{d-1}{2}}^{\frac{d-1}{2}} f''(i,j) k(n-i, m-j) \quad (5)$$

Where f" (i,j) is the result of applying smoothing.

BM technique

After having improved the quality of B-mode images by adjusting the biophysical parameters, we injected them into a BM algorithm. The basic of BM method is to cut the reference image into pixels blocks [18].

For each blocks, a search area is defined in the target image. A resemblance criterion is used to find the best block candidate in a search area. We give their expressions for a ROI size: $L_1 \times L_2$.

Centered on the pixel with coordinates P=(P1, P2) in the reference image. The displacement between a candidate block and the reference ROI is denoted d=(d1, d2) and is bounded by the size of the search area. The position of the best candidate block is denoted, $\left(\hat{d}_1, \hat{d}_2\right)$ [19]. The best candidate corresponds to the maximum of the inter-correlation coefficient (CC).

$$CC(P,d) = \sum_{x_1=-\frac{L_1}{2}}^{\frac{L_1}{2}} \sum_{x_2=-\frac{L2}{2}}^{\frac{L_2}{2}} i_1(P_1+x_1, P_2+x_2).i_2(P_1+x_1+d_1, P_2+x_2+d_2) \quad (6)$$

With $\left(\hat{d}_1, \hat{d}_2\right) = \operatorname{argmax}_d \left(CC(P,d)\right)$ (7)

Results

The evaluations of tissues displacements estimation were performed by three experienced breast radiologists. 20 B-mode images with breast malignant tumors were performed, using high definition linear probe (bandwidth, 15 MHz).

The process described in Section Methods is assessed here; during the process of B-mode images acquisition, we have varied each biophysical parameter value alone, keeping fixed values of the other basic biophysical parameters, that to analyze the impact of each parameter on the B-mode images quality. During the variation of biophysical parameters, quantitative measurements including CNR and SNR were performed.

We have presented the SNR results of the rejection parameter impact in Table 1, for 20 breast B-mode images. CNR and SNR results of the persistence parameter impact for 20 breast B-mode images were presented respectively in Tables 2 and 3.

The CNR and SNR results of smoothing parameter impact for 20 breast B-mode images were presented respectively in Tables 4 and 5.

The radiologist applies a small compression of the breast, with adjustment of the biophysical parameters, after that, the radiologist selects two B-mode images (taken before and after compression), in order to be integrated into the BM model and estimate locally the displacements field. The results were validated by three radiologists. We have presented below the results of the proposed method for improvement of breast tissues displacements estimation (Figures 1-20).

In order to quantitatively compare the efficiency and robustness of our proposed method. We compare it to OBM and BDBM methods, using SD (in pixels) between estimated and B-mode post compression images (as shown in Table 6), CNR comparison (as demonstrated in Table 7), PSNR comparison (as presented in Table 8), and SSIM comparison (as exposed in Table 9), were used to demonstrate the contribution of our proposed method in the improvement of tissues displacement estimation results, and to compare its effectiveness and accuracy with OBM and BDBM approaches.

	Rejection parameter values			
	1	**2**	**3**	**4**
SNR : patient 1	0.85	0.88	0.90	0.90
SNR : patient 2	0.81	0.84	0.87	0.87
SNR : patient 3	0.28	0.31	0.34	0.34
SNR : patient 4	0.59	0.63	0.67	0.67
SNR : patient 5	0.49	0.55	0.57	0.57
SNR : patient 6	0.80	0.91	0.97	0.97
SNR : patient 7	0.81	0.83	0.86	0.86
SNR : patient 8	0.61	0.67	0.71	0.71
SNR : patient 9	0.85	0.89	0.99	0.99
SNR : patient 10	0.75	0.77	0.81	0.81
SNR : patient 11	0.47	0.51	0.59	0.59
SNR : patient 12	0.77	0.81	0.88	0.88
SNR : patient 13	0.71	0.82	0.89	0.89
SNR : patient 14	0.65	0.71	0.77	0.77
SNR : patient 15	0.82	0.89	0.92	0.92
SNR : patient 16	0.91	0.97	1.01	1.01
SNR : patient 17	0.68	0.72	0.72	0.72
SNR : patient 18	0.71	0.73	0.76	0.76
SNR : patient 19	0.64	0.68	0.69	0.69
SNR : patient 20	0.81	0.84	0.87	0.87

Table 1: Impact of the rejection parameter on the SNR results for 20 patients.

	Persistence parameter values									
	1	2	3	4	5	6	7	8	9	10
CNR patient: 1	0.20	0.23	0.30	0.31	0.37	0.40	0.43	0.50	0.51	0.51
CNR patient: 2	0.18	0.19	0.20	0.21	0.24	0.25	0.26	0.28	0.30	0.30
CNR patient: 3	0.24	0.26	0.27	0.31	0.32	0.34	0.35	0.37	0.39	0.39
CNR patient: 4	0.17	0.19	0.21	0.24	0.25	0.26	0.28	0.29	0.33	0.34
CNR patient: 5	0.23	0.25	0.30	0.31	0.33	0.35	0.37	0.37	0.38	0.38
CNR patient: 6	0.19	0.22	0.23	0.27	0.28	0.33	0.34	0.35	0.37	0.37
CNR patient: 7	0.15	0.16	0.18	0.22	0.23	0.25	0.28	0.29	0.32	0.32
CNR patient: 8	0.22	0.24	0.25	0.26	0.27	0.29	0.31	0.32	0.34	0.34
CNR patient: 9	0.23	0.24	0.30	0.31	0.32	0.34	0.39	0.40	0.43	0.43
CNR patient: 10	0.16	0.20	0.21	0.23	0.24	0.27	0.29	0.30	0.35	0.35
CNR patient: 11	0.18	0.19	0.21	0.24	0.27	0.29	0.32	0.33	0.36	0.36
CNR patient: 12	0.23	0.24	0.25	0.27	0.33	0.34	0.37	0.38	0.39	0.39
CNR patient: 13	0.18	0.19	0.21	0.24	0.25	0.27	0.31	0.32	0.37	0.37
CNR patient: 14	0.16	0.18	0.19	0.22	0.29	0.31	0.32	0.33	0.36	0.36
CNR patient: 15	0.11	0.13	0.15	0.16	0.19	0.22	0.26	0.27	0.29	0.29
CNR patient: 16	0.14	0.17	0.18	0.19	0.22	0.23	0.25	0.26	0.32	0.32
CNR patient: 17	0.17	0.19	0.22	0.23	0.24	0.25	0.27	0.27	0.28	0.28
CNR patient: 18	0.22	0.23	0.24	0.26	0.27	0.31	0.32	0.33	0.35	0.35
CNR patient: 19	0.31	0.32	0.35	0.36	0.37	0.40	0.41	0.42	0.44	0.44
CNR patient: 20	0.24	0.27	0.28	0.29	0.31	0.33	0.38	0.39	0.41	0.41

Table 2: Impact of the persistence parameter on the CNR results for 20 patients.

	Persistence parameter values									
	1	2	3	4	5	6	7	8	9	10
SNR patient: 1	0.90	0.91	0.94	0.99	1.10	1.20	1.40	1.69	1.70	1.70
SNR patient: 2	0.87	0.88	0.91	0.94	0.96	0.97	0.98	1.11	1.14	1.13
SNR patient: 3	0.34	0.36	0.37	0.39	0.42	0.44	0.45	0.50	0.51	0.50
SNR patient: 4	0.67	0.68	0.71	0.72	0.73	0.76	0.80	0.91	0.93	0.92
SNR patient: 5	0.57	0.58	0.60	0.61	0.64	0.67	0.68	0.73	0.77	0.76
SNR patient: 6	0.97	0.98	1	1.10	1.13	1.15	1.18	1.20	1.24	1.24
SNR patient: 7	0.86	0.87	0.89	0.91	0.92	0.96	0.97	1.13	1.19	1.15
SNR patient: 8	0.71	0.74	0.75	0.79	0.81	0.82	0.84	0.91	0.94	0.93
SNR patient: 9	0.99	1	1.13	1.17	1.18	1.19	1.23	1.27	1.31	1.31
SNR patient: 10	0.81	0.84	0.85	0.87	0.88	0.93	0.95	1.12	1.16	1.15
SNR patient: 11	0.59	0.61	0.62	0.65	0.69	0.76	0.78	0.85	0.88	0.86
SNR patient: 12	0.88	0.91	0.93	0.94	0.98	0.99	1	1.13	1.19	1.15
SNR patient: 13	0.89	0.93	0.94	0.99	1	1.14	1.17	1.32	1.35	1.33
SNR patient: 14	0.77	0.78	0.81	0.82	0.86	0.87	0.91	1.01	1.12	1.11
SNR patient: 15	0.92	0.95	0.98	0.99	1	1.13	1.17	1.31	1.34	1.34
SNR patient: 16	1.01	1.13	1.17	1.20	1.26	1.27	1.30	1.42	1.45	1.44
SNR patient: 17	0.72	0.73	0.74	0.77	0.78	0.81	0.84	0.89	1	0.91
SNR patient: 18	0.76	0.77	0.80	0.83	0.84	0.85	0.88	1.31	1.35	1.35
SNR patient: 19	0.69	0.73	0.74	0.77	0.79	0.81	0.82	1.14	1.17	1.16
SNR patient: 20	0.87	0.88	0.91	0.93	0.94	0.95	0.98	1.23	0.41	0.41

Table 3: Impact of the persistence parameter on the SNR results for 20 patients.

Discussion

In order to objectively compare the results presented in "*In-vivo* breast images" section, we can evaluate the breast tissue displacement estimation improvement based on the quantitative indicators. As mentioned in the previous sections, we used an ultrasound B-mode images database of breast organ corresponding to 20 patients with malignant tumor, all results have been verified and validated by three radiologists.

We simulate our proposed method on the ultrasound images, and we compared it to both methods (OBM and BDBM methods), as it was expected, the best accuracy of tissues displacements estimation was obtained when the proposed approach is applied.

The proposed approach provides more accurate tissue displacements estimation with good tumor detection and tissues localization than OBM and BDBM techniques. The proposed method also provides a greater reduction in noise and a higher resolution in pixels than that obtained by the other two methods. The tissue displacements estimation images, obtained with our proposed model, appears very clear resulting in increased sharpness, the distinction between homogeneous region pixels and those of an outline are well plotted, we notice also an increased improvement in preservation of contours, with good clarity in less contrasting areas.

	Smoothing parameter values				
	1	**2**	**3**	**4**	**5**
CNR patient: 1	0.51	0.53	0.55	0.58	0.58
CNR patient: 2	0.30	0.34	0.39	0.42	0.42
CNR patient: 3	0.39	0.44	0.45	0.47	0.47
CNR patient: 4	0.33	0.37	0.38	0.43	0.43
CNR patient: 5	0.38	0.39	0.41	0.47	0.47
CNR patient: 6	0.37	0.40	0.43	0.44	0.44
CNR patient: 7	0.32	0.37	0.38	0.49	0.49
CNR patient: 8	0.34	0.35	0.37	0.46	0.46
CNR patient: 9	0.43	0.44	0.45	0.53	0.53
CNR patient: 10	0.35	0.37	0.39	0.47	0.47
CNR patient: 11	0.36	0.39	0.42	0.56	0.56
CNR patient: 12	0.39	0.42	0.43	0.45	0.45
CNR patient: 13	0.37	0.39	0.42	0.47	0.47
CNR patient: 14	0.36	0.43	0.46	0.52	0.52
CNR patient: 15	0.29	0.35	0.39	0.49	0.49
CNR patient: 16	0.32	0.33	0.38	0.47	0.47
CNR patient: 17	0.28	0.33	0.36	0.48	0.48
CNR patient: 18	0.35	0.37	0.43	0.54	0.54
CNR patient: 19	0.44	0.46	0.47	0.50	0.50
CNR patient: 20	0.41	0.44	0.49	0.53	0.53

Table 4: Impact of the smoothing parameter on the CNR results for 20 patients.

	Smoothing parameter values				
	1	**2**	**3**	**4**	**5**
SNR patient: 1	1.70	1.73	1.74	1.77	1.77
SNR patient: 2	1.14	1.15	1.19	1.32	1.32
SNR patient: 3	0.51	0.55	0.83	0.92	0.92
SNR patient: 4	0.93	1.12	1.19	1.26	1.26
SNR patient: 5	0.77	0.93	1.13	1.23	1.23
SNR patient: 6	1.24	1.43	1.49	1.64	1.64
SNR patient: 7	1.19	1.34	1.41	1.52	1.52
SNR patient: 8	0.94	1.26	1.30	1.49	1.49
SNR patient: 9	1.31	1.52	1.53	1.62	1.62
SNR patient: 10	1.16	1.19	1.23	1.34	1.34
SNR patient: 11	0.88	0.92	1.14	1.19	1.19
SNR patient: 12	1.19	1.23	1.27	1.37	1.37
SNR patient: 13	1.35	1.39	1.42	1.55	1.55
SNR patient: 14	1.12	1.17	1.18	1.32	1.32
SNR patient: 15	1.34	1.38	1.39	1.41	1.41
SNR patient: 16	1.45	1.46	1.51	1.55	1.55
SNR patient: 17	1	1.21	1.23	1.29	1.29
SNR patient: 18	1.35	1.37	1.39	1.46	1.46
SNR patient: 19	1.17	1.18	1.21	1.26	1.26
SNR patient: 20	0.41	0.44	0.49	0.53	0.53

Table 5: Impact of the smoothing parameter on the SNR results for 20 patients.

The proposed strategy that it used to improve the quality of tissue displacements estimation images, acts by coupling the biophysical parameters with the BM model, the results are surely improved.

Our proposed model consists of two parts: The first part, studies the biophysical parameters improving the quality of B-mode images; the second part, implements the improved B-mode images into a displacement estimation algorithm: BM. In order to study the impact of proposed biophysical approach, we calculated the quantitative criteria (CNR and SNR) related to B-mode images.

It can be observed from Table 1, that the rejection function parameter makes it possible to take only the data containing more information than the other, a configuration of this parameter to a value equal to 3, makes us to obtain a high SNR in B-mode images.

This is explained by the fact that the rejection filter, selects only the noise-free autocorrelations or otherwise, it does not allow the passage of the band frequency containing the parasitic noise. Each increase of the rejection parameter indicates a decrease in the cut-off frequency of the filter which selects signals that are free of noise.

A parameterization of the rejection function at value equal to 3, parameterizes the filter to eliminate speckle noise deteriorating the

	OBM method	BDBM method	Proposed method
SD in pixels: Patient 1	7.12	6.41	5.23
SD in pixels: Patient 2	6.43	5.32	4.18
SD in pixels: Patient 3	5.20	4.91	3.72
SD in pixels: Patient 4	9.31	8.54	7.81
SD in pixels: Patient 5	8.11	6.71	5.67
SD in pixels: Patient 6	9.17	8.99	8.31
SD in pixels: Patient 7	6.11	4.56	4.39
SD in pixels: Patient 8	5.23	4.38	3.87
SD in pixels: Patient 9	7.20	5.72	4.13
SD in pixels: Patient 10	7.76	4.85	3.98
SD in pixels: Patient 11	8.91	6.72	5.14
SD in pixels: Patient 12	9.22	8.42	7.32
SD in pixels: Patient 13	9.76	7.81	6.71
SD in pixels: Patient 14	7.31	6.91	5.87
SD in pixels: Patient 15	5.71	4.51	3.88
SD in pixels: Patient 16	8.56	6.80	5.61
SD in pixels: Patient 17	7.19	5.79	4.94
SD in pixels: Patient 18	10.31	7.18	6.73
SD in pixels: Patient 19	9.81	8.43	7.18
SD in pixels: Patient 20	7.65	5.77	4.31

Table 6: *In vivo* results comparison of SD in pixels for the proposed method with OBM and BDBM methods for 20 patients.

	B-mode image	OBM method	BDBM method	Proposed method
CNR : Patient 1	0.31	0.34	0.39	0.54
CNR : Patient 2	1.62	1.88	1.97	2.12
CNR : Patient 3	0.62	0.79	1.12	1.20
CNR : Patient 4	1.14	1.32	1.75	1.98
CNR : Patient 5	0.74	0.87	1.16	1.62
CNR : Patient 6	0.16	0.54	1.09	1.13
CNR : Patient 7	1.23	1.56	1.70	1.82
CNR : Patient 8	0.18	0.63	0.89	1.10
CNR : Patient 9	0.95	1.11	1.74	1.98
CNR : Patient 10	0.19	0.34	0.40	0.73
CNR : Patient 11	0.53	0.77	0.93	1.31
CNR : Patient 12	0.61	0.89	1.16	1.39
CNR : Patient 13	0.73	1.32	1.64	1.85
CNR : Patient 14	0.39	0.65	0.73	1.13
CNR : Patient 15	0.41	0.61	0.70	1.20
CNR : Patient 16	0.72	0.84	0.92	1.51
CNR : Patient 17	0.87	0.95	1.09	1.18
CNR : Patient 18	0.74	0.99	1.13	1.62
CNR : Patient 19	0.73	1.01	1.23	1.76
CNR : Patient 20	0.39	0.75	1.23	1.59

Table 7: Comparison of CNR for the proposed method with OBM and BDBM methods for 20 patients.

quality of images, a value greater than 3, has no effect. This stage is very important, since it only passes signals of very high value in SNR.

It is seen from Tables 2 and 3, that the persistence has improved the CNR and SNR results of B-mode images quality when the value is set at 9; thanks to the use of spatial filtering applied by the persistence. It has ensured a good reduction of the noise. A value greater than 9 has no effect on image quality, therefore a parameterization of the filter in value equal to 9, improves significantly both CNR and SNR and provides a good visualization of the mammary structures in the variation scale of persistence parameter.

From Tables 4 and 5, the smoothing parameter showed a good correction of the rapid transitions of the noise in image especially when setting the filter value at 4, thanks to the use of the low pass filter which has attenuated strongly the noise and artifacts in the image and has improved the two quantitative parameters of CNR and SNR.

The configuration of the biophysical parameters to the mentioned values allows optimizing the B-mode images quality by improving their CNR and SNR Criteria. At this stage, the displacement estimation algorithm is ready to be coupled.

The proposed method was compared with the BM and BDBM methods, using quantitative and qualitative criteria, which aims to validate the effectiveness of our strategy.

The tissue displacement estimation obtained by our proposed strategy, BM and BDBM methods are presented in Figures 1-20. Our

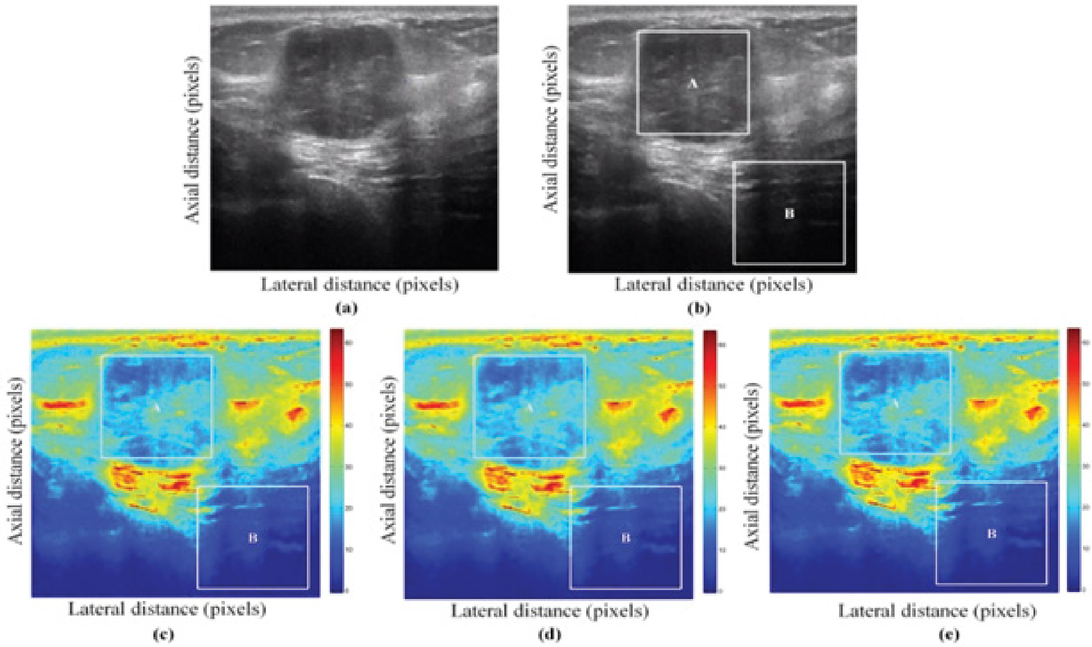

Figure 1: Estimating tissue displacements of breast malignant tumor for the patient. **A** Simulated pre compression B-mode image. **B** Simulated post compression B-mode image. **C** tissues displacement obtained with OBM method. **D** tissues displacement obtained with BDBM method, and **E** tissues displacement obtained with proposed method: Areas selected by a rectangle are used for mathematical computation.

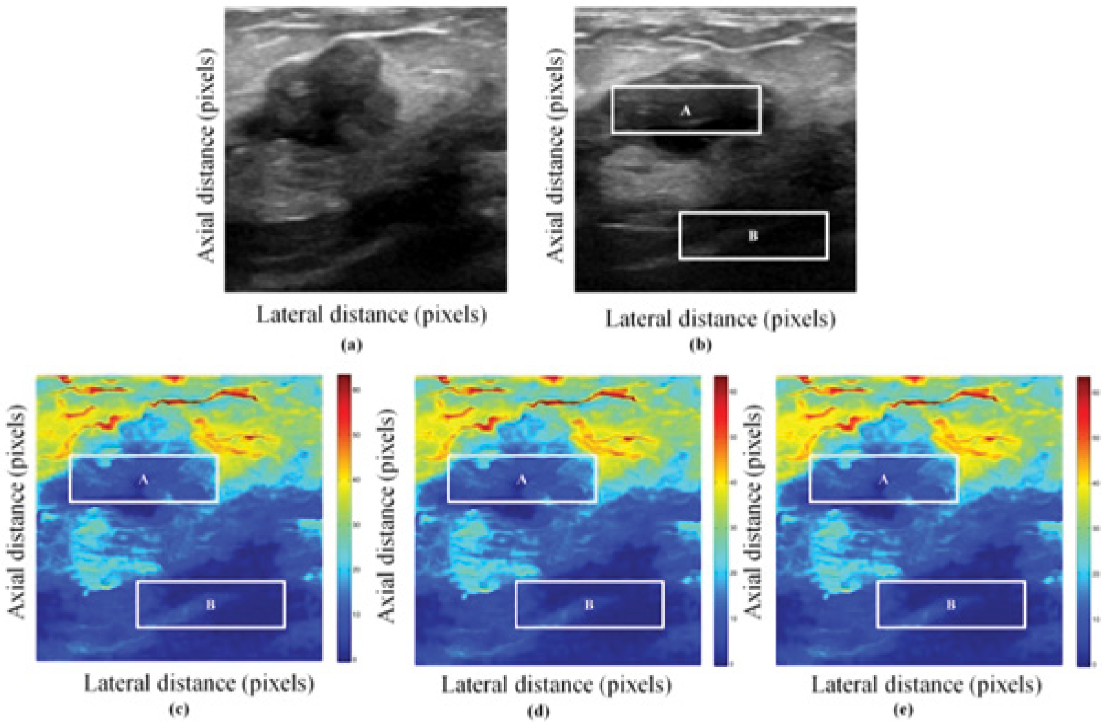

Figure 2: Estimating tissue displacements of breast malignant tumor for the patient. **A** Simulated pre compression B-mode image. **B** Simulated post compression B-mode image. **C** tissues displacement obtained with OBM method. **D** tissues displacement obtained with BDBM method, and **E** tissues displacement obtained with proposed method: Areas selected by a rectangle are used for mathematical computation.

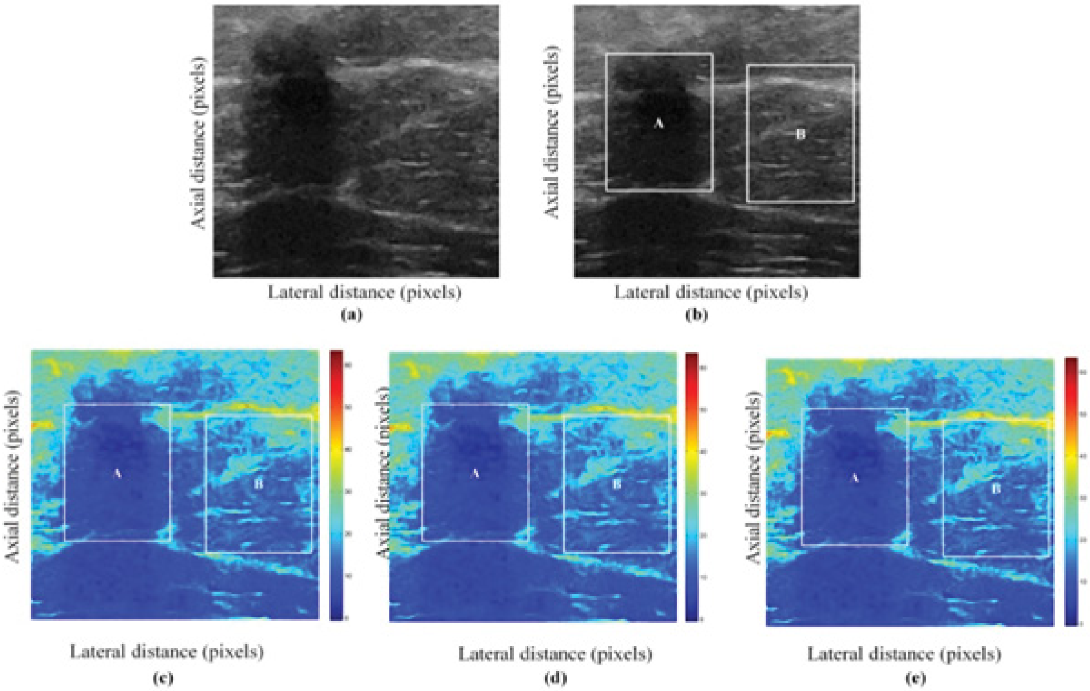

Figure 3: Estimating tissue displacements of breast malignant tumor for the patient. **A** Simulated pre compression B-mode image. **B** Simulated post compression B-mode image. **C** tissues displacement obtained with OBM method. **D** tissues displacement obtained with BDBM method, and **E** tissues displacement obtained with proposed method: Areas selected by a rectangle are used for mathematical computation.

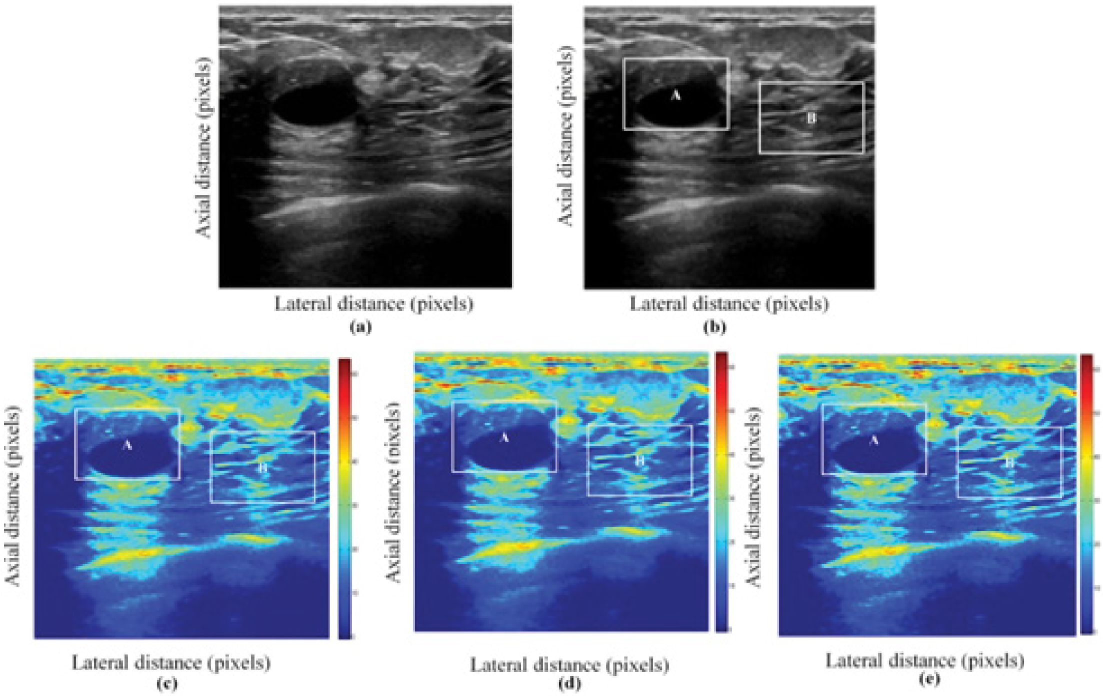

Figure 4: Estimating tissue displacements of breast malignant tumor for the patient. **A** Simulated pre compression B-mode image. **B** Simulated post compression B-mode image. **C** tissues displacement obtained with OBM method. **D** tissues displacement obtained with BDBM method, and **E** tissues displacement obtained with proposed method: Areas selected by a rectangle are used for mathematical computation.

Citation: Slimi T, Tamali R, Mahjoubi H (2019) Enhancement of Displacement Estimation of Breast Tissue in Ultrasound Elastography. J Tissue Sci Eng 9: 223. doi: 10.4172/2157-7552.1000223

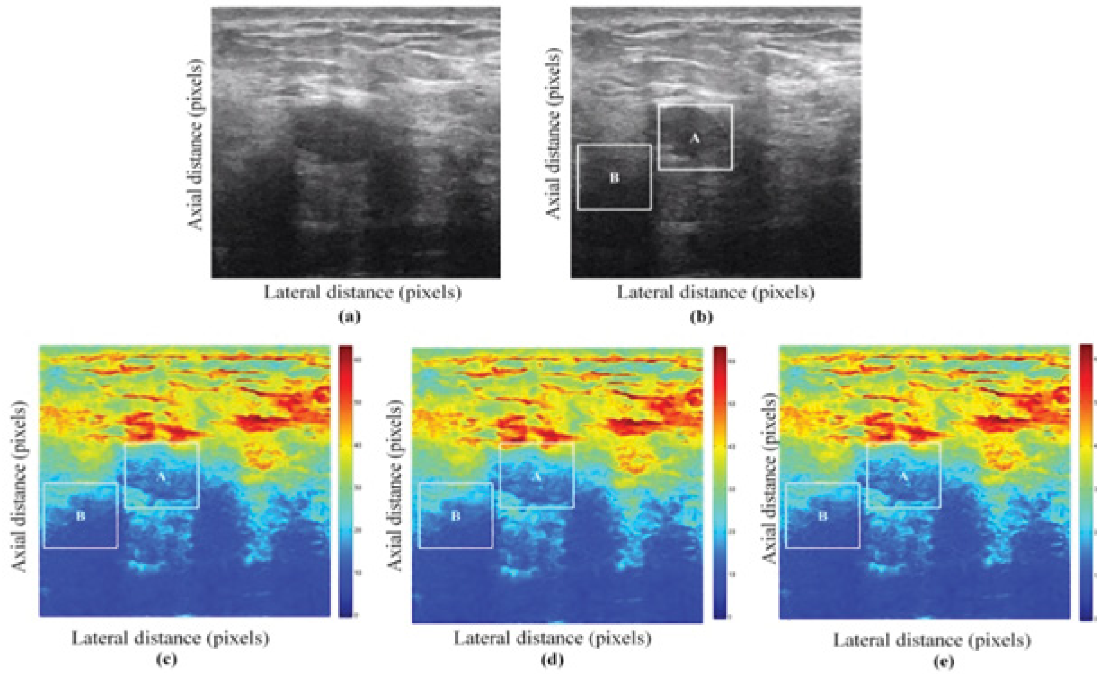

Figure 5: Estimating tissue displacements of breast malignant tumor for the patient. **A** Simulated pre compression B-mode image. **B** Simulated post compression B-mode image. **C** tissues displacement obtained with OBM method. **D** tissues displacement obtained with BDBM method, and **E** tissues displacement obtained with proposed method: Areas selected by a rectangle are used for mathematical computation.

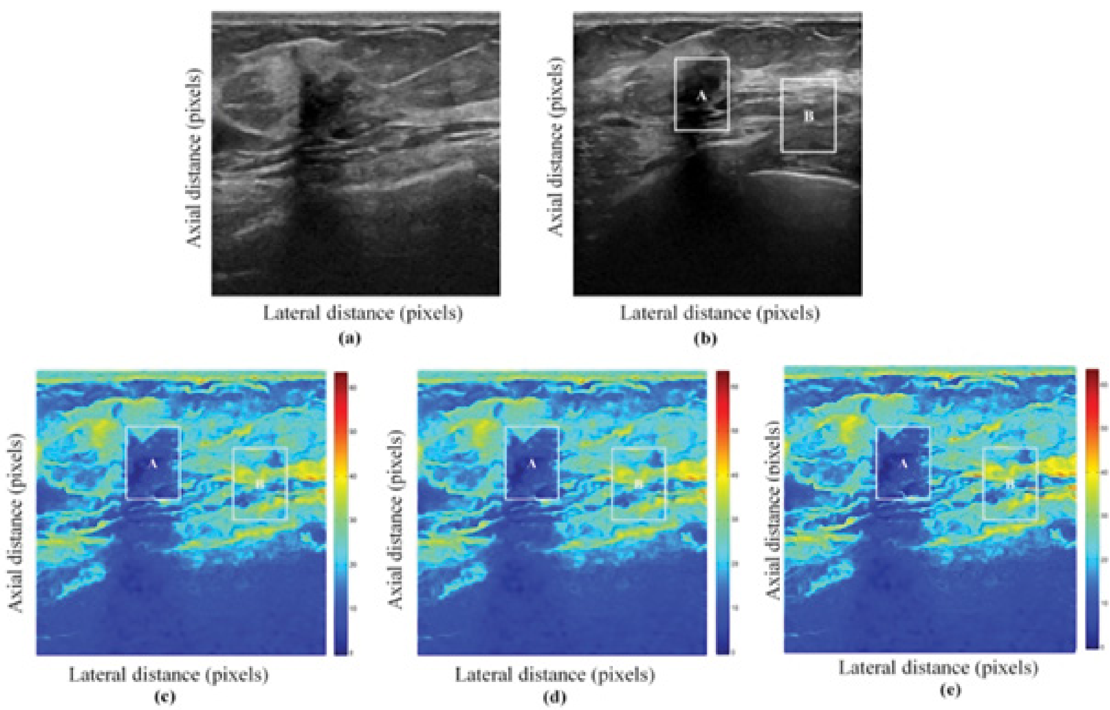

Figure 6: Estimating tissue displacements of breast malignant tumor for the patient. **A** Simulated pre compression B-mode image. **B** Simulated post compression B-mode image. **C** tissues displacement obtained with OBM method. **D** tissues displacement obtained with BDBM method, and **E** tissues displacement obtained with proposed method: Areas selected by a rectangle are used for mathematical computation.

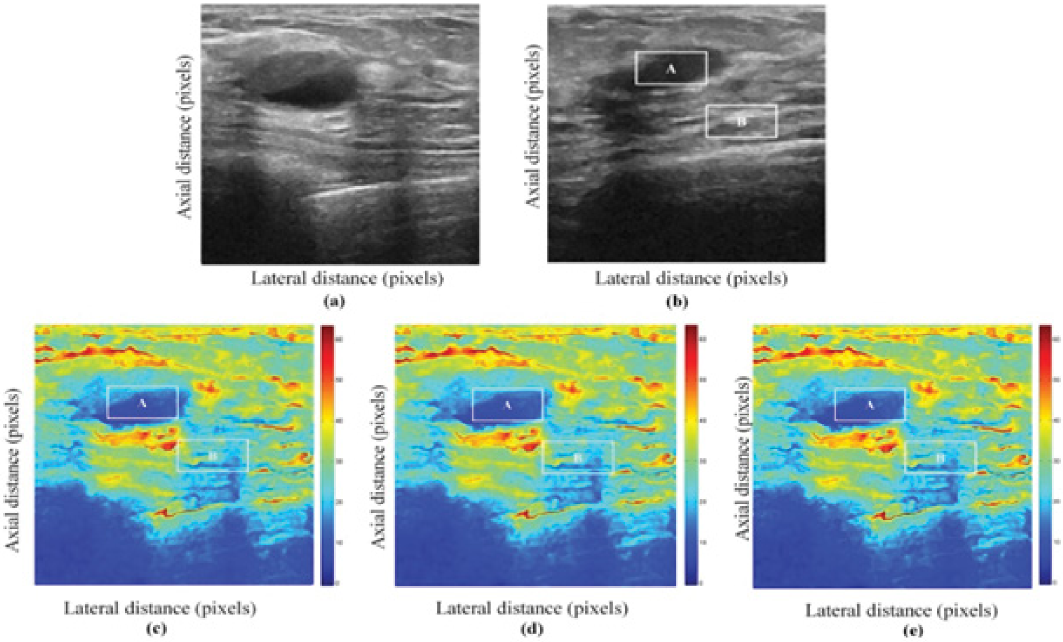

Figure 7: Estimating tissue displacements of breast malignant tumor for the patient. **A** Simulated pre compression B-mode image. **B** Simulated post compression B-mode image. **C** tissues displacement obtained with OBM method. **D** tissues displacement obtained with BDBM method, and **E** tissues displacement obtained with proposed method: Areas selected by a rectangle are used for mathematical computation.

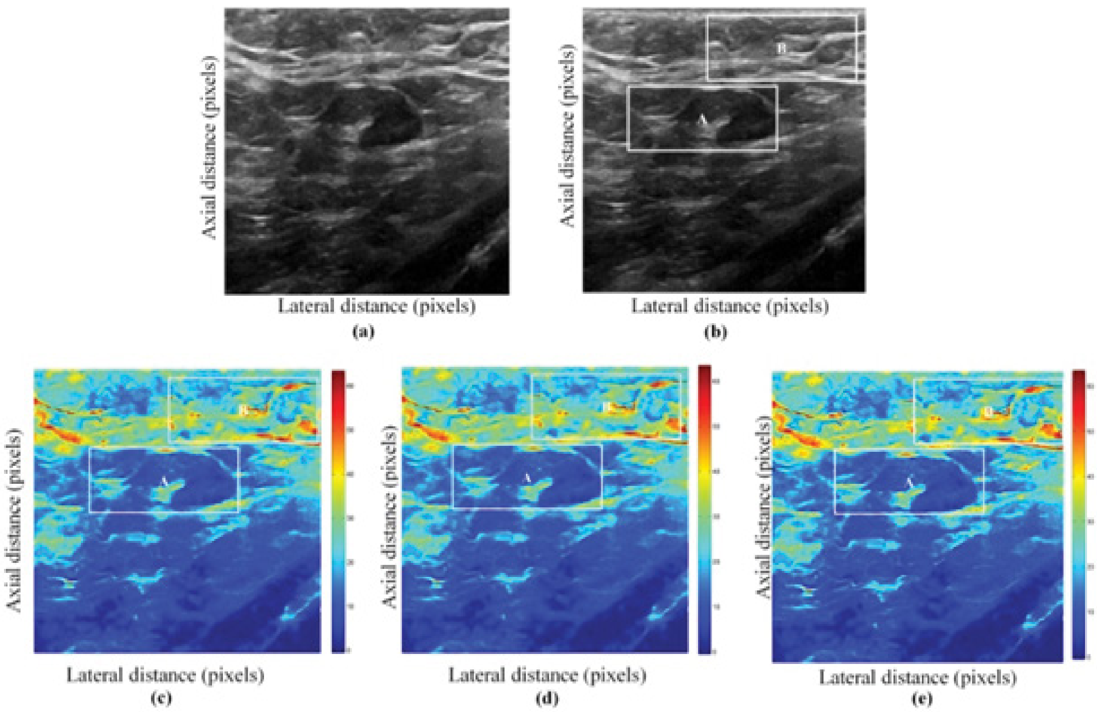

Figure 8: Estimating tissue displacements of breast malignant tumor for the patient. **A** Simulated pre compression B-mode image. **B** Simulated post compression B-mode image. **C** tissues displacement obtained with OBM method. **D** tissues displacement obtained with BDBM method, and **E** tissues displacement obtained with proposed method: Areas selected by a rectangle are used for mathematical computation.

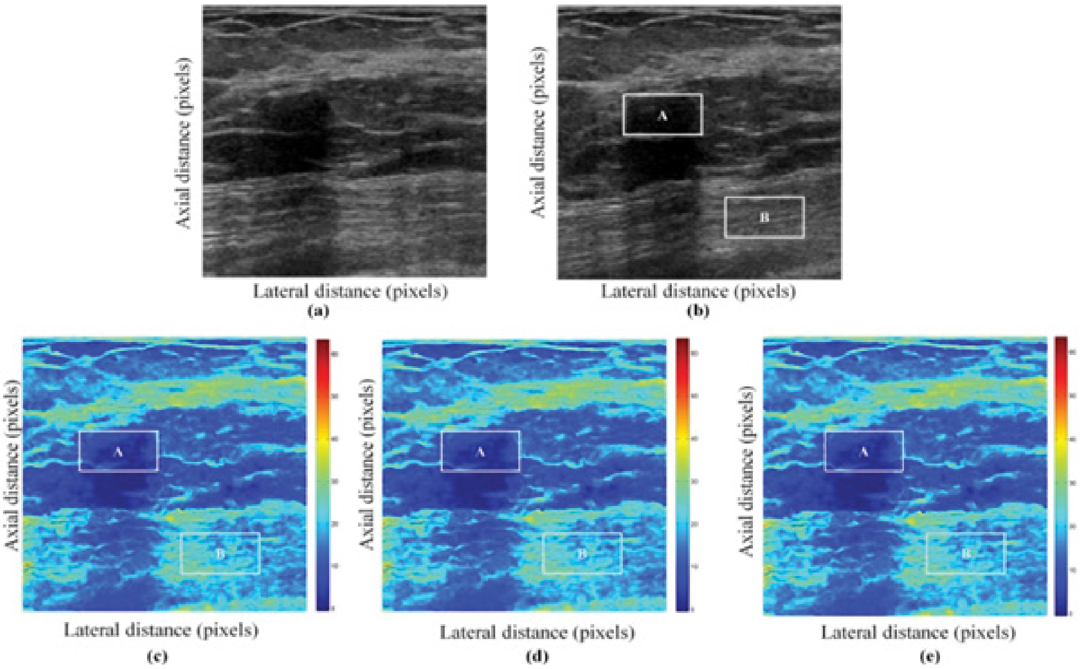

Figure 9: Estimating tissue displacements of breast malignant tumor for the patient. **A** Simulated pre compression B-mode image. **B** Simulated post compression B-mode image. **C** tissues displacement obtained with OBM method. **D** tissues displacement obtained with BDBM method, and **E** tissues displacement obtained with proposed method: Areas selected by a rectangle are used for mathematical computation.

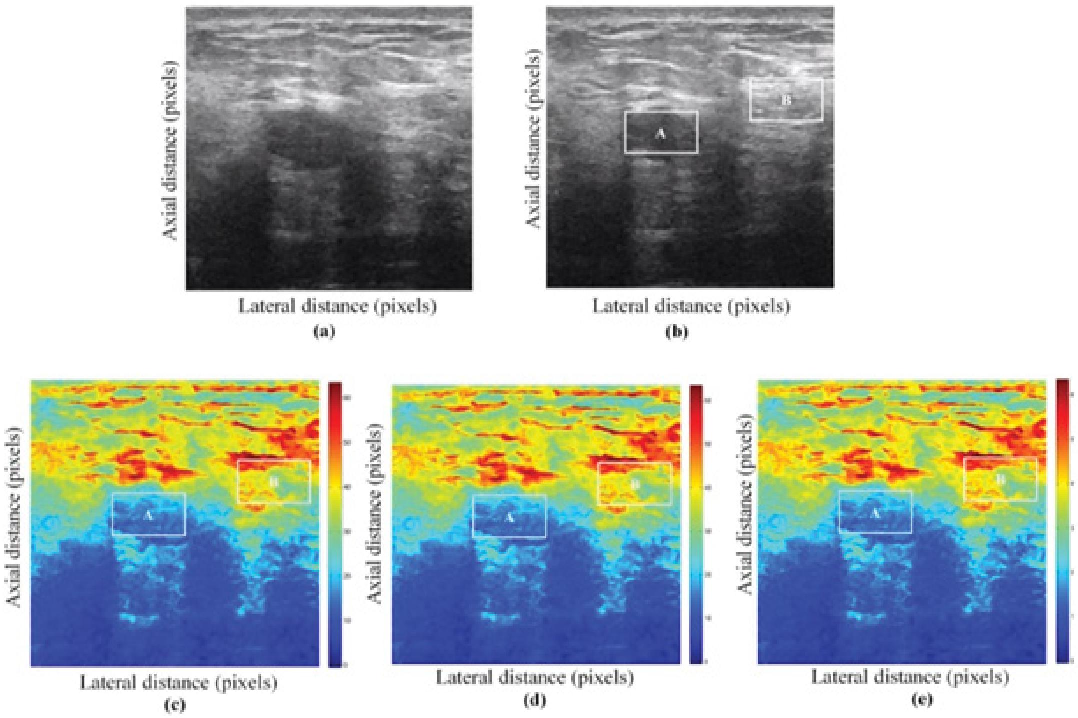

Figure 10: Estimating tissue displacements of breast malignant tumor for the patient. **A** Simulated pre compression B-mode image. **B** Simulated post compression B-mode image. **C** tissues displacement obtained with OBM method. **D** tissues displacement obtained with BDBM method, and **E** tissues displacement obtained with proposed method: Areas selected by a rectangle are used for mathematical computation.

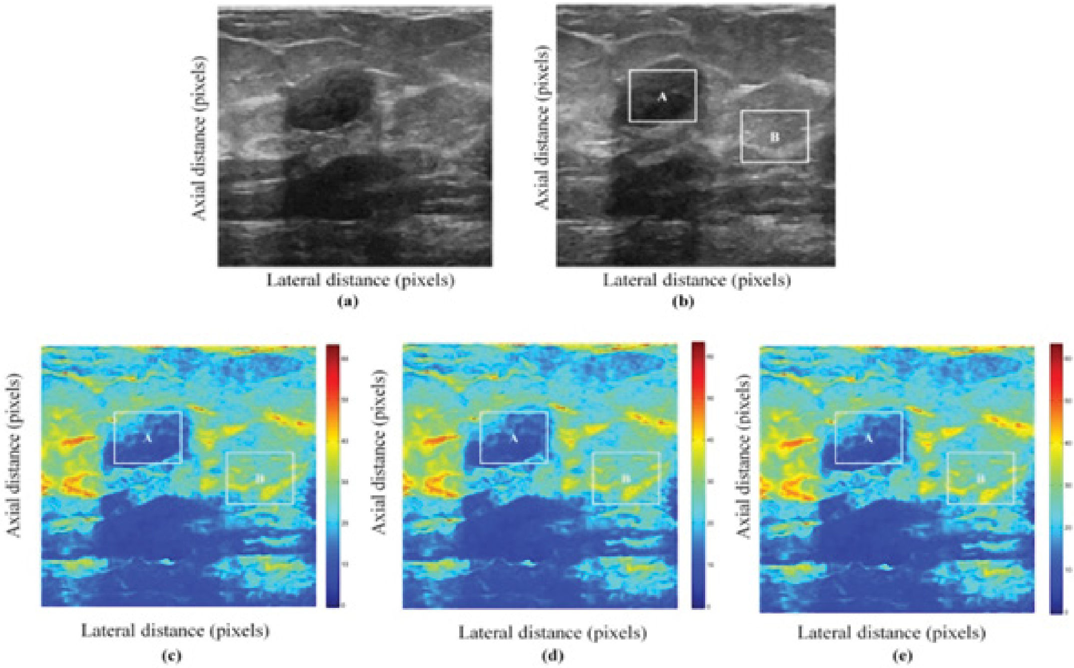

Figure 11: Estimating tissue displacements of breast malignant tumor for the patient. **A** Simulated pre compression B-mode image. **B** Simulated post compression B-mode image. **C** tissues displacement obtained with OBM method. **D** tissues displacement obtained with BDBM method, and **E** tissues displacement obtained with proposed method: Areas selected by a rectangle are used for mathematical computation.

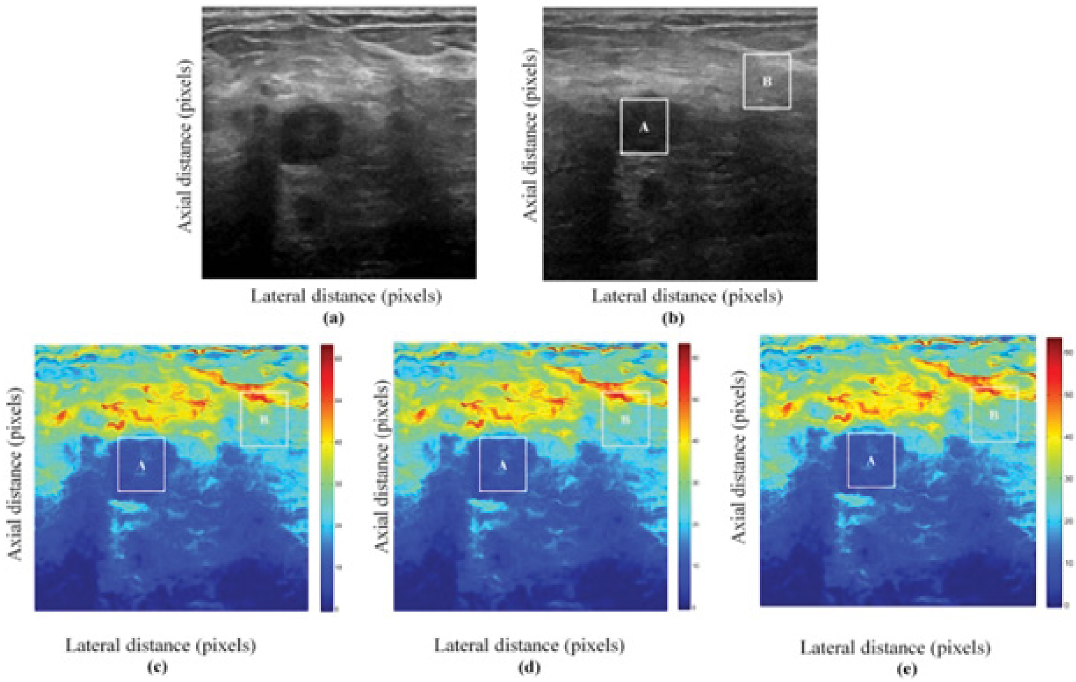

Figure 12: Estimating tissue displacements of breast malignant tumor for the patient. **A** Simulated pre compression B-mode image. **B** Simulated post compression B-mode image. **C** tissues displacement obtained with OBM method. **D** tissues displacement obtained with BDBM method, and **E** tissues displacement obtained with proposed method: Areas selected by a rectangle are used for mathematical computation.

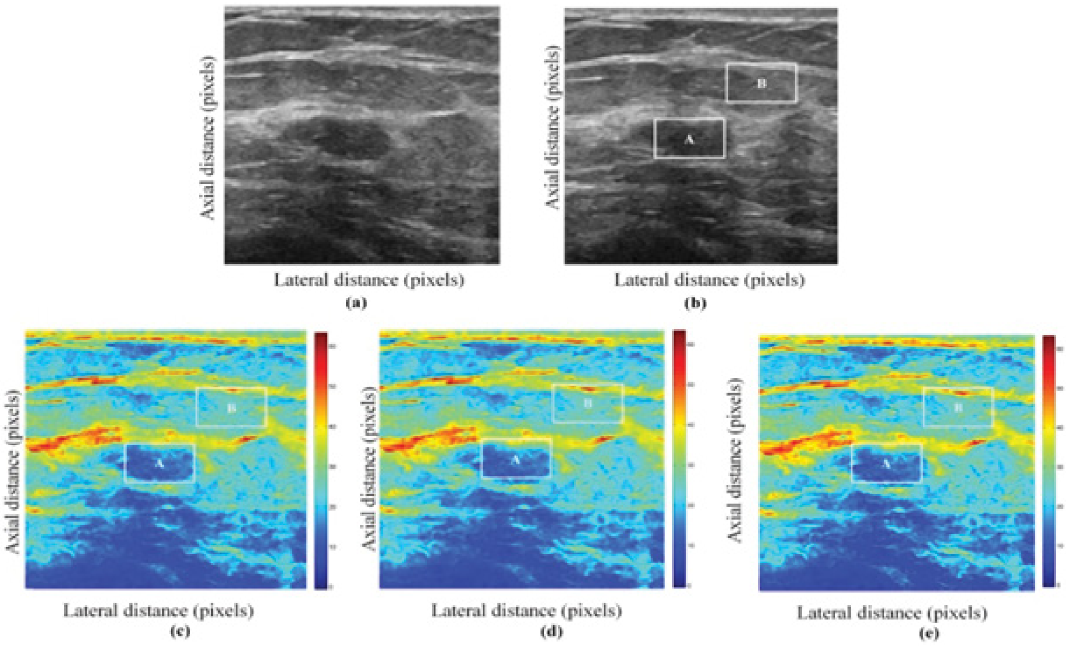

Figure 13: Estimating tissue displacements of breast malignant tumor for the patient. **A** Simulated pre compression B-mode image. **B** Simulated post compression B-mode image. **C** tissues displacement obtained with OBM method. **D** tissues displacement obtained with BDBM method, and **E** tissues displacement obtained with proposed method: Areas selected by a rectangle are used for mathematical computation.

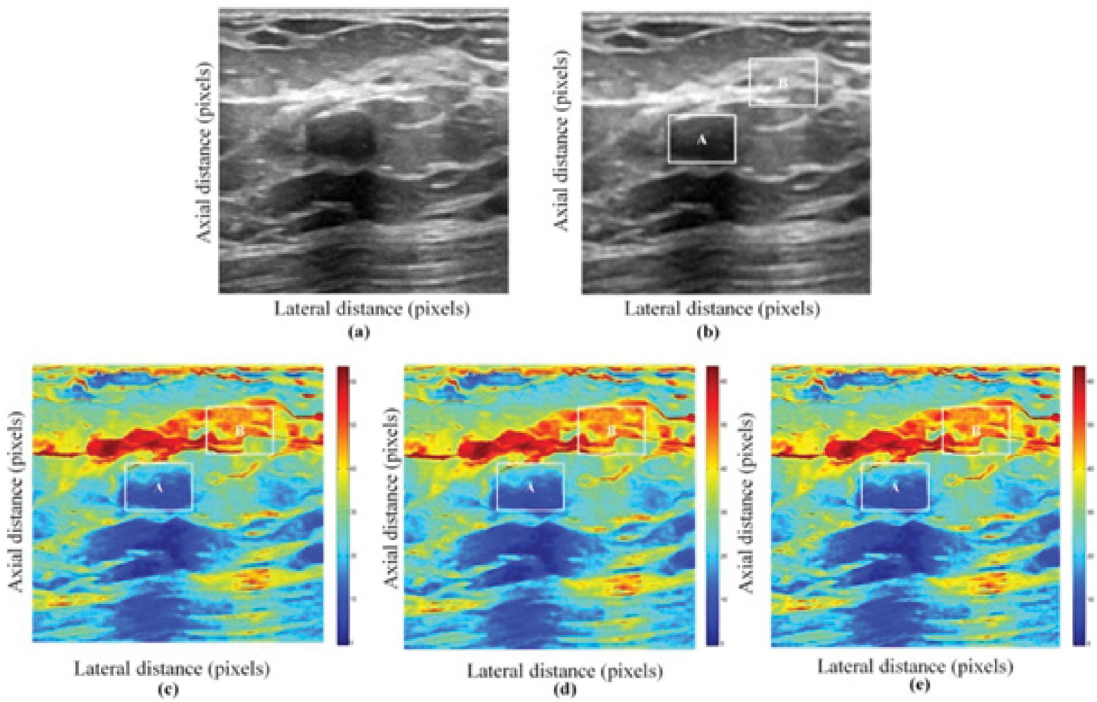

Figure 14: Estimating tissue displacements of breast malignant tumor for the patient. **A** Simulated pre compression B-mode image. **B** Simulated post compression B-mode image. **C** tissues displacement obtained with OBM method. **D** tissues displacement obtained with BDBM method, and **E** tissues displacement obtained with proposed method: Areas selected by a rectangle are used for mathematical computation.

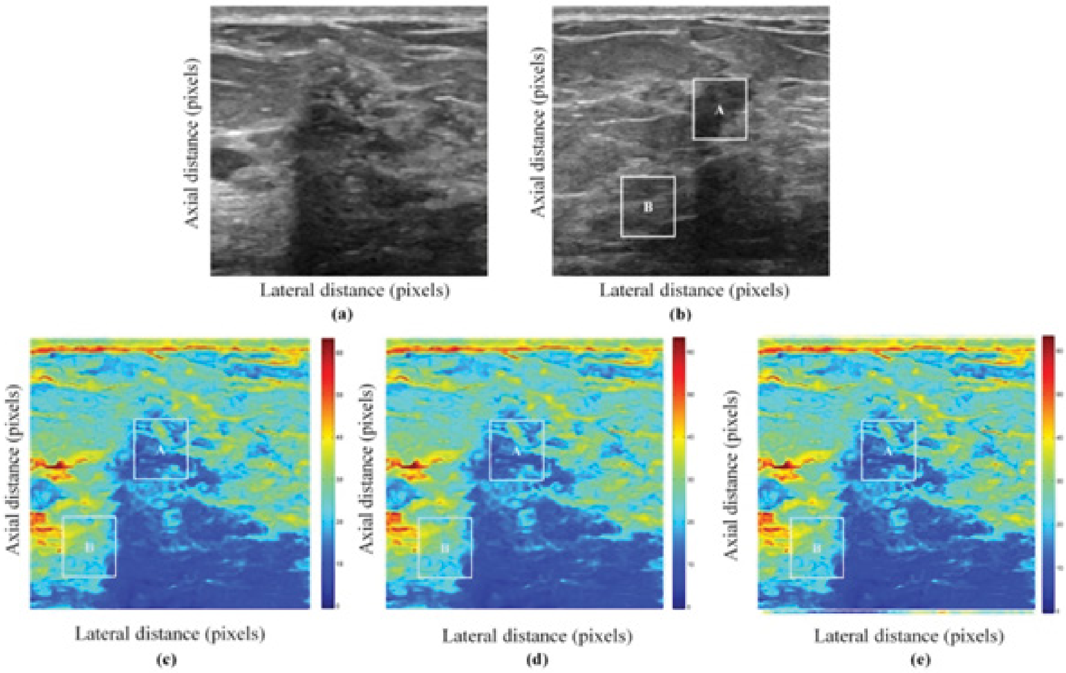

Figure 15: Estimating tissue displacements of breast malignant tumor for the patient. **A** Simulated pre compression B-mode image. **B** Simulated post compression B-mode image. **C** tissues displacement obtained with OBM method. **D** tissues displacement obtained with BDBM method, and **E** tissues displacement obtained with proposed method: Areas selected by a rectangle are used for mathematical computation.

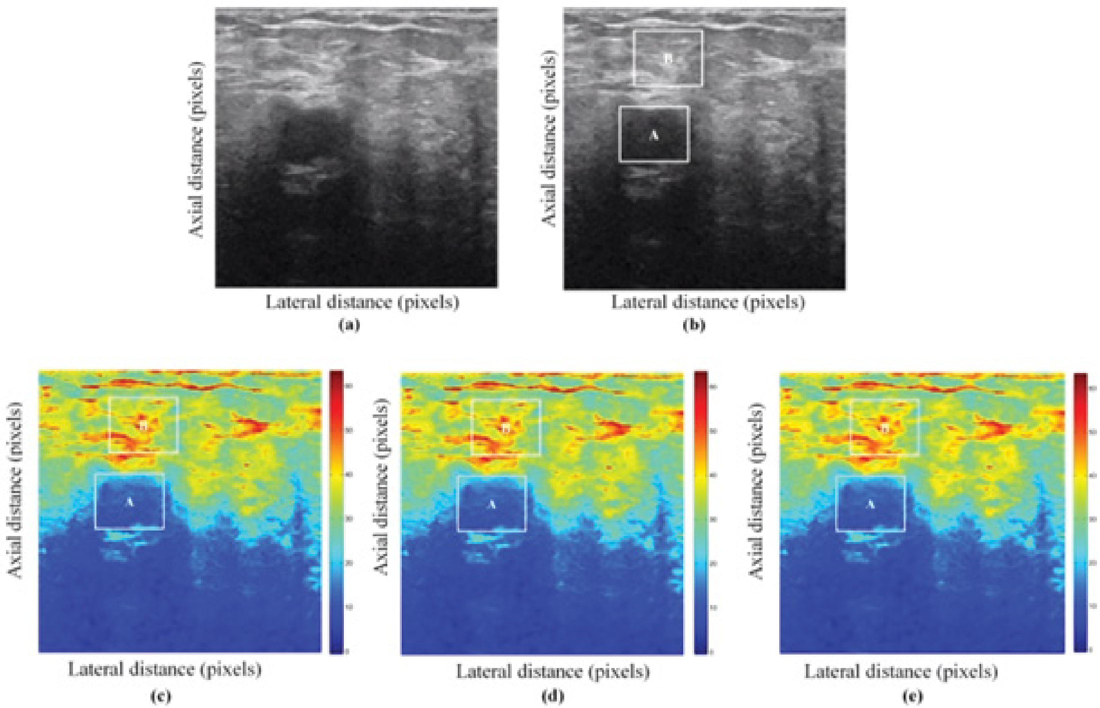

Figure 16: Estimating tissue displacements of breast malignant tumor for the patient. **a** Simulated pre compression B-mode image. **b** Simulated post compression B-mode image. **c** tissues displacement obtained with OBM method. **d** tissues displacement obtained with BDBM method, and **e** tissues displacement obtained with proposed method: Areas selected by a rectangle are used for mathematical computation.

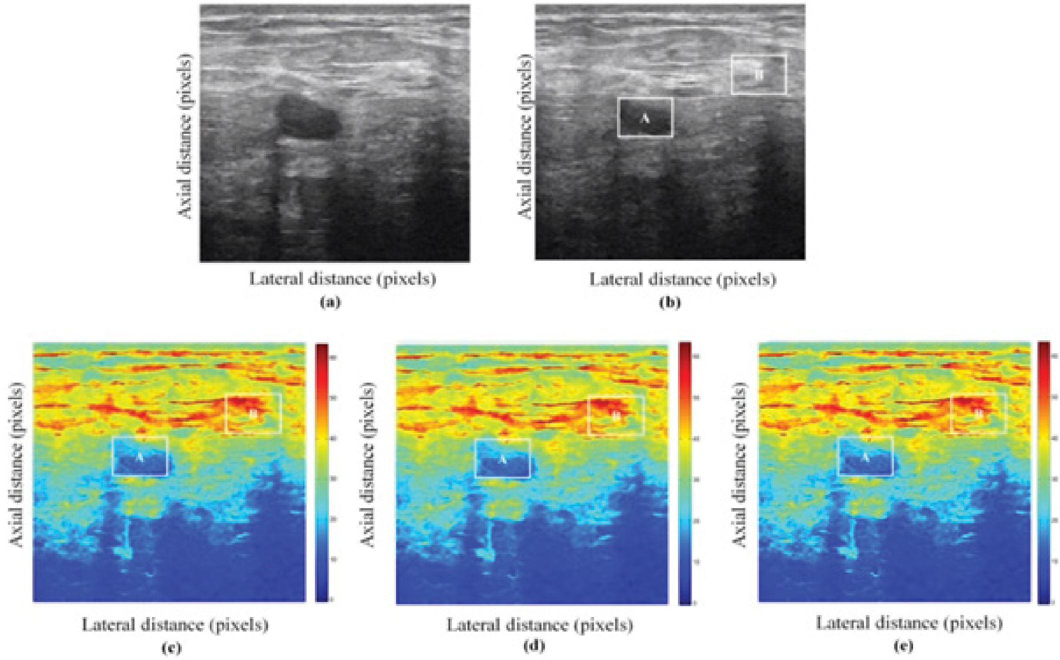

Figure 17: Estimating tissue displacements of breast malignant tumor for the patient. **A** Simulated pre compression B-mode image. **B** Simulated post compression B-mode image. **C** tissues displacement obtained with OBM method. **D** tissues displacement obtained with BDBM method, and **E** tissues displacement obtained with proposed method: Areas selected by a rectangle are used for mathematical computation.

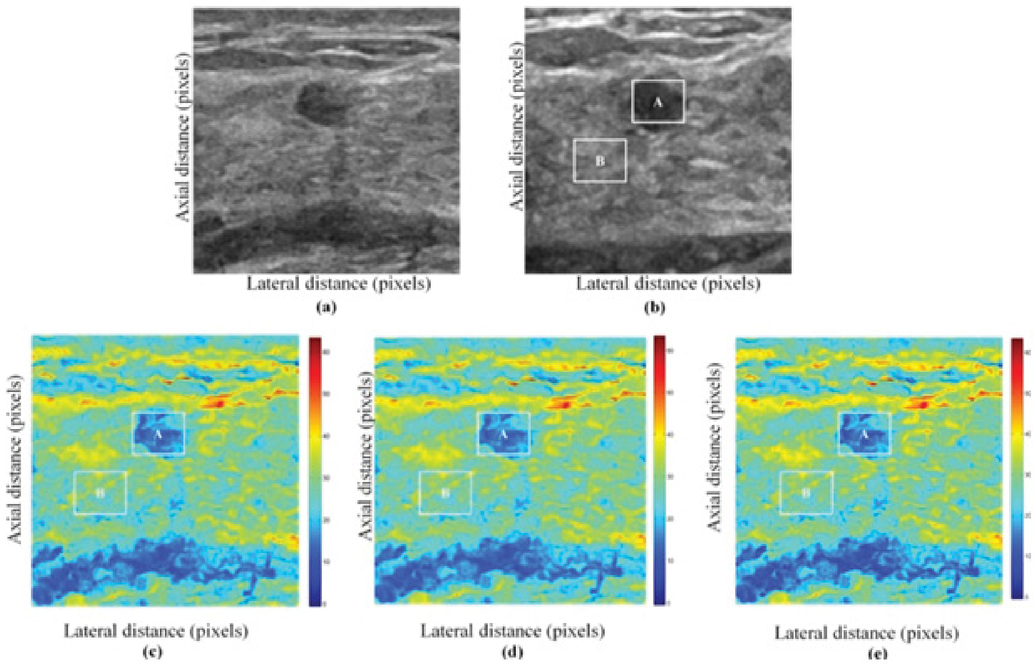

Figure 18: Estimating tissue displacements of breast malignant tumor for the patient. **A** Simulated pre compression B-mode image. **B** Simulated post compression B-mode image. **C** tissues displacement obtained with OBM method. **D** tissues displacement obtained with BDBM method, and **E** tissues displacement obtained with proposed method: Areas selected by a rectangle are used for mathematical computation.

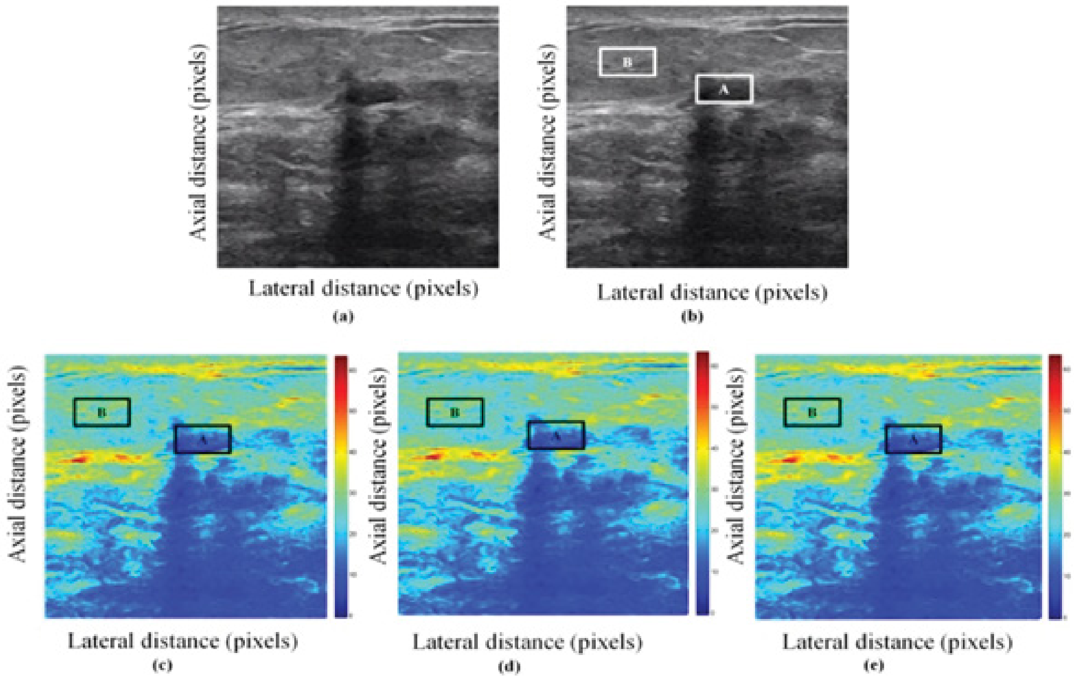

Figure 19: Estimating tissue displacements of breast malignant tumor for the patient. **A** Simulated pre compression B-mode image. **B** Simulated post compression B-mode image. **C** tissues displacement obtained with OBM method. **D** tissues displacement obtained with BDBM method, and **E** tissues displacement obtained with proposed method: Areas selected by a rectangle are used for mathematical computation.

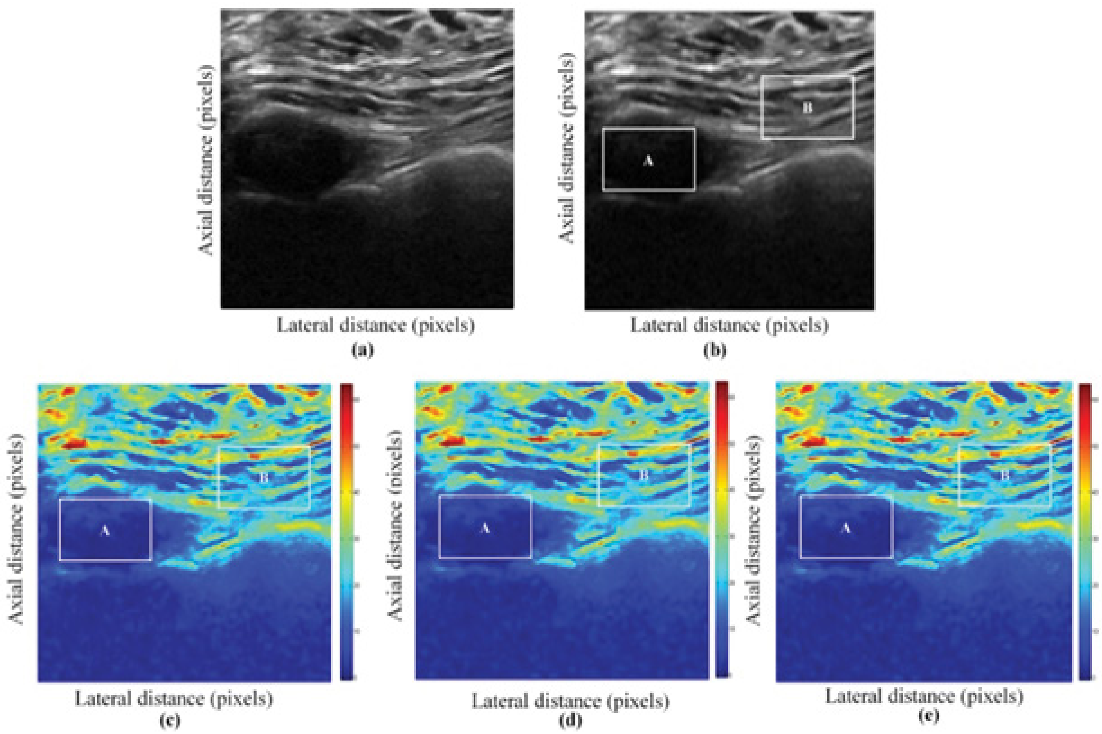

Figure 20: Estimating tissue displacements of breast malignant tumor for the patient. **A** Simulated pre compression B-mode image. **B** Simulated post compression B-mode image. **C** tissues displacement obtained with OBM method. **D** tissues displacement obtained with BDBM method, and **E** tissues displacement obtained with proposed method: Areas selected by a rectangle are used for mathematical computation.

	OBM method	BDBM method	Proposed method
PSNR : Patient 1	19.50	21.71	27.87
PSNR : Patient 2	10.72	13.81	15.31
PSNR : Patient 3	19.30	23.49	30.12
PSNR : Patient 4	11.23	15.43	18.73
PSNR : Patient 5	28.91	32.40	42.61
PSNR : Patient 6	10.51	13.10	15.42
PSNR : Patient 7	28.71	32.87	34.85
PSNR : Patient 8	23.55	27.65	31.53
PSNR : Patient 9	32.76	34.71	38.91
PSNR : Patient 10	25.81	28.11	32.65
PSNR : Patient 11	15.67	18.10	23.85
PSNR : Patient 12	26.78	30.04	35.61
PSNR : Patient 13	9.94	11.31	15.83
PSNR : Patient 14	30.83	34.71	39.17
PSNR : Patient 15	38.45	42.18	48.73
PSNR : Patient 16	19.73	22.91	27.82
PSNR : Patient 17	16.84	18.73	20.33
PSNR : Patient 18	19.93	21.61	29.35
PSNR : Patient 19	20.11	22.32	27.19
PSNR : Patient 20	28.71	30.21	34.91

Table 8: Comparison of PSNR for the proposed method with OBM and BDBM methods for 20 patients.

	OBM method	BDBM method	Proposed method
SSIM : Patient 1	0.70	0.76	0.84
SSIM : Patient 2	0.56	0.72	0.81
SSIM : Patient 3	0.87	0.90	0.94
SSIM : Patient 4	0.45	0.64	0.70
SSIM : Patient 5	0.27	0.52	0.81
SSIM : Patient 6	0.68	0.71	0.80
SSIM : Patient 7	0.79	0.83	0.91
SSIM : Patient 8	0.65	0.70	0.74
SSIM : Patient 9	0.51	0.64	0.75
SSIM : Patient 10	0.60	0.71	0.87
SSIM : Patient 11	0.81	0.85	0.91
SSIM : Patient 12	0.69	0.72	0.80
SSIM : Patient 13	0.55	0.63	0.70
SSIM : Patient 14	0.61	0.69	0.78
SSIM : Patient 15	0.86	0.92	0.95
SSIM : Patient 16	0.52	0.66	0.71
SSIM : Patient 17	0.71	0.74	0.87
SSIM : Patient 18	0.41	0.56	0.67
SSIM : Patient 19	0.30	0.41	0.59
SSIM : Patient 20	0.79	0.82	0.91

Table 9: Comparison of SSIM for the proposed method with OBM and BDBM methods for 20 patients.

proposed approach offers a better estimation results and good tumor localization with better visibility of the contours than that obtained by BM and BDBM methods.

In order to numerically evaluate the results assessment, we calculated the SD, CNR, PSNR, and SSIM for each method.

From Table 6, it can be seen that the proposed method gets the lowest SD in pixels value: On one hand, the proposed method is an improved model based on the biophysical optimization of B-mode images coupled with BM model, and the tissue displacement estimation results also show that the proposed strategy performs better than OBM technique.

On the other, compared with BDBM technique, the proposed method obtains a strong de-speckling ability, greater improvement of displacement estimation and more satisfactory result.

The filtering of B-mode images is not accessible for the other methods (OBM and BDBM techniques) since no filtering is applied, which has induced a noisy displacements estimation images [20,21]. In this context, the error will be very great for OBM and BDBM techniques. This explains the smaller SD value in the proposed model.

From Table 7, The CNRs values are calculated and presented for each patient. The first CNR is calculated using the gray levels of the B-mode images. The other three CNRs are calculated from the results of BM, BDBM and proposed methods. By analyzing these results, we observe that although the CNR is good in BM and BDBM techniques, our approach offers a better contrast between the healthy parts and the tumor tissues. The CNR reports confirm that when we used our proposed approach, the tumor is best discriminated on breast tissue displacements. The improvement in CNR in our proposed method is largely due to the removal of artifacts and speckle noise from neighboring breast tissue. Therefore, the degree of contrast enhancement will be related to the acquisition of B-mode images.

The contrast enhancement will be maximized when the two B-mode images (pre and post compression) are better recorded in terms of biophysical parameter adjustment. If the biophysical parameters are not perfectly adjusted during B-mode image acquisition, speckle noise cancellation will not be complete and residual artifacts from tissue compression may persist.

From Table 8, it is shown that the PSNR of the BM technique is still at a very low level due to its inability to filter image, since this approach directly estimates the tissue displacements without taking into account the presence of speckle noise. The BDBM technique also does not give a good PSNR values, since in this method; no filter is present: neither for image denoising nor for details conservation. While in the case of our proposed method, the existence of biophysical approach in the B-mode image processing step, has greatly improved the resolution of displacement estimation image, and perfectly reduces the noise.

It is seen from Table 9, that the proposed method has surpassed the other methods with the highest SSIM value. The BM technique has the lowest SSIM value and this is very expected, since this method suffers from the presence of speckle noise and does not preserve the details of tissue displacements estimation. Also, the BDBM technique has lower SSIM values than that obtained by our proposed model; this is explained by the fact that the BDBM technique estimates the tissue displacement without prior treatment of B-mode image.

With our strategy, we obtained more impressive results with a strongly improved SSIM; the idea of image processing by biophysical parameterization mentioned above has succeeded to improve the SSIM criterion. The proposed method is the most reliable process algorithm in majority suppression of noise by retaining the details in displacement estimation images. The SSIM results confirm that our technique created for the displacements estimation improvement is an appropriate combination for ultrasound elastography compared to the OBM and BDBM methods.

In this article, we have improved the OBM technique used in quasi-static breast ultrasound elastography; we have exploited the impact of biophysical parameters, coupled with BM model to ensure a satisfactory optimization of tissue displacements estimation results. We have set up a new technique that can efficiently enhance the breast tissue displacement estimation performance.

The proposed technique will overcome the problems encountered in elastography; it will solve several complications, related to the deterioration and disappearance of details, in areas with low contrast. The implementation of our new strategy will help doctors for accurate diagnostic reports for the evaluation of breast malignant tumor elasticity.

Conclusion

In this paper, a new strategy is proposed for the improvement of breast tissue displacements estimation, the employed strategy has perfected the OBM technique used in breast strain estimation in ultrasound elastography. The new profit of our proposed concept helps to improve the diagnosis of breast tumor.

A biophysical approach including rejection, persistence and smoothing parameters were implemented during B-mode images acquisition and combined with BM model, which aims to improve the breast tissue displacement estimation.

This method is very efficient in strain estimation, it is not only has a strong de-speckling ability, but also it estimates tissue displacement with high accuracy.

In addition, the adaptation of biophysical parameters with BM model constituting the purpose of our proposed method was discussed. The accuracy of our new strategy was tested on *In-vivo* ultrasound images using 20 patients with malignant tumors.

It has been shown that our proposed strategy performs better compared to OBM and BDBM techniques, provided better SD, greater CNR, higher PSNR and more suitable SSIM than OBM and BDBM techniques. Therefore, the proposed method provides encouraging, supportive, exciting results and it will be a significant support for effective diagnosis of breast diseases.

Widely, the proposed optimization strategy is advantageous for improving the tissue displacements estimation of Breast ultrasound elastography, for better diagnosis of mammary pathologies.

Declaration Section

Ethics approval and consent to participate

The radiology department of the Hospital University Monji Slim Marsa and the Laboratory of Biophysics and Medical Technology Research declare agreement on ethical approval and consent: 20 images without the names of patients (anonymous) contain malignant tumors in the breast. The ethics committee of the laboratory of Biophysics and Medical Technologies, reference number LR13ES07 has approved the study. Written informed report was obtained from the patients for publication of this manuscript and accompanying images.

Consent for Publication

Not applicable.

Acknowledgements

The authors would like to thank the doctors teams of the university hospital of Monji Slim, Tunisia, for providing and assessing the clinical Breast data.

References

1. Cho N, Jang M, Lyou CY, Park JS, Choi HY, et al. (2012) Distinguishing benign from malignant masses at breast US: Combined US elastography and color Doppler US-influence on radiologist accuracy. Radiology 262: 80-90.
2. Gu P, Lee WM, Roubidoux MA, Yuan J, Wang X, et al. (2016) Automated 3D ultrasound image segmentation to aid breast cancer image interpretation. Ultrasonics 65: 51-58.
3. Slimi T, Moussa I, Kraiem T, Mahjoubi H (2017) Estimation of Displacement Tissues in Breast Ultrasound Elastography. J Diagn Tech Biomed Anal 6: 1.
4. Tsigginou A, Gkali C, Chalazonitis A, Feida E, Efthymios D, et al. (2016) Adding the power of iodinated contrast media to the credibility of mammography in breast cancer diagnosis. Br J Radiol 89: 1067-1069.
5. Xiao Y, Yu Y, Niu L, Qiana M, Denga Z, et al. (2016) Quantitative evaluation of peripheral tissue elasticity for ultrasound-detected breast lesions. Clin Radiol 71: 896-904.
6. Slimi T, Moussa IM, Kraiem T, Mahjoubi H (2017) Improvement of displacement estimation of breast tissue in ultrasound elastography using the monogenic signal. Biomed Eng Online 16: 19.

7. DiBattista A, Noble JA (2014) An efficient block matching and spectral shift estimation algorithm with applications to ultrasound elastography. IEEE Trans Ultrason Ferroelectr Freq Control 61: 407-419.

8. Maltaverne T, Delachartre P, Basarab A (2010) Motion estimation using the monogenic signal applied to ultrasound elastography. Conf Proc IEEE Eng Med Biol Soc 2010: 33-36.

9. Slimi T, Moussa I, Kraiem T, Mahjoubi H (2017) Improvement of Breast Elastogram Quality in Static Ultrasound Elastography using Biophysical Parameters. J Diagn Tech Biomed Anal 6.

10. Thomas A, Kummel S, Fritzsche F, Warmd M, Eberte B, et al. (2006) Real-time sonoelastography performed in addition to B-mode ultrasound and mammography: Improved differentiation of breast lesions. Acad Radiol 13: 1496-1504.

11. Xiao X, Jiang Q, Wu H, Guan X, Qin W, et al. (2017) Diagnosis of sub-centimetre breast lesions: combining BI-RADS-US with strain elastography and contrast-enhanced ultrasound-a preliminary study in China. Eur Radiol 27: 2443-2450.

12. Eisenbrey JR, Dave JK, Forsberg F (2016) Recent technological advancements in breast ultrasound. Ultrasonics 70: 183-190.

13. Cheng Y, Yunjie J, Shengdi W, Long Li, Mushuang H, et al. (2016) Prediction of Renal Allograft Acute Rejection Using a Novel Non-Invasive Model Based on Acoustic Radiation Force Impulse. Ultrasound Med Biol 42: 2167-2179.

14. Kuzmin A, Zakrzewski AM, Anthony BW, Lempitsky V (2015) Multi-frame elastography using a handheld force-controlled ultrasound probe. IEEE Trans Ultrason Ferroelectr Freq Control 62: 1486-1500.

15. Filoux E, Mamou J, Ketterling JA, Aristizabal O (2010) Estimation of spatial resolution for high-frequency imaging systems using a novel anechoic-sphere phantom. J Acoust Soc Am 128: 2280.

16. Han Y, Kim DW, Kwon HJ (2012) Application of digital image cross-correlation and smoothing function to the diagnosis of breast cancer. J Mech Behav Biomed Mater 14: 7-18.

17. Kwon HJ, Lee J (2014) Low-cost quasi-real-time elastography using B-mode ultrasound images. Biomed Mater Eng 24: 1673-1692.

18. Zhou Y, Zheng YP (2010) A motion estimation refinement framework for real-time tissue axial strain estimation with freehand ultrasound. IEEE Trans Ultrason Ferroelectr Freq Control 57: 1943-1951.

19. Wang X, Mitchell CC, Varghese T, Jackson DC, Rocque BG, et al. (2016) Improved Correlation of Strain Indices with Cognitive Dysfunction with Inclusion of Adventitial Layer with Carotid Plaque. Ultrason Imaging 38:194-208.

20. Basarab A, Gueth P, Liebgott H, Delachartre P (2009) Phase-based block matching applied to motion estimation with unconventional beamforming strategies. IEEE Trans Ultrason Ferroelectr Freq Control 56: 945-957.

21. Basarab A, Gueth P, Liebgott H, Delachartre P (2007) Two-dimensional least-squares estimation for motion tracking in ultrasound elastography. Conf Proc IEEE Eng Med Biol Soc 2007: 2155-2158.